



## $\mathcal{PT}$ Metamaterials via Complex-Coordinate Transformation Optics

Giuseppe Castaldi,<sup>1</sup> Silvio Savoia,<sup>1</sup> Vincenzo Galdi,<sup>1,\*</sup> Andrea Alù,<sup>2</sup> and Nader Engheta<sup>3</sup>

<sup>1</sup>*Waves Group, Department of Engineering, University of Sannio, I-82100 Benevento, Italy*

<sup>2</sup>*Department of Electrical and Computer Engineering, The University of Texas at Austin, Austin, Texas 78712, USA*

<sup>3</sup>*Department of Electrical and Systems Engineering, University of Pennsylvania, Philadelphia, Pennsylvania 19104, USA*

(Received 29 October 2012; revised manuscript received 18 January 2013; published 23 April 2013)

We extend the transformation-optics paradigm to a complex spatial coordinate domain, in order to deal with electromagnetic metamaterials characterized by balanced loss and gain, giving special emphasis to parity-time ( $\mathcal{PT}$ ) symmetric metamaterials. We apply this general theory to complex-source-point radiation and anisotropic transmission resonances, illustrating the capability and potentials of our approach in terms of systematic design, analytical modeling, and physical insights into complex-coordinate wave objects and resonant states.

DOI: [10.1103/PhysRevLett.110.173901](https://doi.org/10.1103/PhysRevLett.110.173901)

PACS numbers: 42.25.Bs, 11.30.Er, 42.70.-a

Balanced loss-gain artificial materials have elicited growing attention in optics and photonics, mostly inspired by the emerging parity-time ( $\mathcal{PT}$ ) symmetry concept, which was originally introduced in connection with quantum physics [1] (see Ref. [2] for a comprehensive review). Against the traditional axioms in quantum mechanics, Bender and co-workers [2] proved that even non-Hermitian Hamiltonians may exhibit entirely real energy eigenspectra, as long as they commute with the combined  $\mathcal{PT}$  operator and share the same eigenstates. This implies, as a necessary condition on the quantum potential,  $V(-\mathbf{r}) = V^*(\mathbf{r})$ , with  $\mathbf{r}$  denoting a vector position and  $*$  indicating complex conjugation.

In view of the formal analogies between Schrödinger and paraxial Helmholtz equations, the above concepts and conditions may be straightforwardly translated to scalar optics and photonics scenarios, with complex-valued refractive-index profiles  $n(-\mathbf{r}) = n^*(\mathbf{r})$  playing the role of the quantum potential. Such symmetry condition cannot be found in natural materials, but it may be engineered within current metamaterial technology, with a judicious spatial modulation of optical gain and losses (either along or across the propagation direction). Besides providing convenient experimental test beds for  $\mathcal{PT}$ -symmetry-induced quantum-field effects that are still a subject of debate,  $\mathcal{PT}$ -symmetric metamaterials constitute *per se* a very intriguing paradigm, as the complex interplay between losses and gain may give rise to a wealth of anomalous, and otherwise unattainable, light-matter interaction effects that extend far beyond the rather intuitive loss (over)compensation effects [3]. These include, for instance, double refraction [4], power oscillations [4,5], spontaneous  $\mathcal{PT}$ -symmetry breaking [6,7], beam switching [8], absorption-enhanced transmission [6], effectively nonreciprocal propagation [9–15], spectral singularities [16], and coherent perfect absorption [17,18], with perspective applications to new-generation optical components, switches, lasers, and absorbers.

In this Letter, we show that the transformation optics (TO) framework [19,20] may be extended, via complex analytic continuation of the spatial coordinates, in order to deal with  $\mathcal{PT}$ -symmetric metamaterials. This extension brings along the powerful TO “bag of tools,” already applied successfully to a wide variety of field-manipulating metamaterials [21], in terms of systematic design, analytical modeling, and valuable physical insights. Our approach may be related to recent efforts in applying the coordinate-transformation methods to quantum mechanics in order to generate classes of exactly solvable  $\mathcal{PT}$ -symmetric potentials (see, e.g., Refs. [22,23] and references therein).

For simplicity, we start by considering an auxiliary vacuum space with Cartesian coordinates  $\mathbf{r}' \equiv (x', y', z')$ , where time-harmonic [ $\exp(-i\omega t)$ ] electric ( $\mathbf{J}'$ ) and magnetic ( $\mathbf{M}'$ ) sources radiate an electromagnetic (EM) field ( $\mathbf{E}'$ ,  $\mathbf{H}'$ ). We then consider a coordinate transformation

$$\mathbf{r}' = \mathbf{F}(\mathbf{r}) \quad (1)$$

into a new curved-coordinate space. By relying on the covariance properties of Maxwell’s equations, the TO framework [20] allows for a “material” interpretation of the field-manipulation effects induced by the coordinate transformation in (1), in terms of a new set of sources ( $\mathbf{J}$ ,  $\mathbf{M}$ ) and fields ( $\mathbf{E}$ ,  $\mathbf{H}$ ) residing in a *flat* physical space  $\mathbf{r} \equiv (x, y, z)$  filled up by an inhomogeneous, anisotropic “transformation medium” (characterized by relative permittivity and permeability tensors  $\underline{\underline{\epsilon}}$  and  $\underline{\underline{\mu}}$ , respectively) that are related to the original quantities as follows

$$\{\mathbf{E}, \mathbf{H}\}(\mathbf{r}) = \underline{\underline{\Lambda}}^T(\mathbf{r}) \cdot \{\mathbf{E}', \mathbf{H}'\}[\mathbf{F}(\mathbf{r})], \quad (2a)$$

$$\{\mathbf{J}, \mathbf{M}\}(\mathbf{r}) = \det[\underline{\underline{\Lambda}}(\mathbf{r})] \underline{\underline{\Lambda}}^{-1}(\mathbf{r}) \cdot \{\mathbf{J}', \mathbf{M}'\}[\mathbf{F}(\mathbf{r})], \quad (2b)$$

$$\underline{\underline{\epsilon}}(\mathbf{r}) = \underline{\underline{\mu}}(\mathbf{r}) = \det[\underline{\underline{\Lambda}}(\mathbf{r})] \underline{\underline{\Lambda}}^{-1}(\mathbf{r}) \cdot \underline{\underline{\Lambda}}^{-T}(\mathbf{r}). \quad (2c)$$

In (2),  $\underline{\underline{\Lambda}} \equiv \partial(x', y', z')/\partial(x, y, z)$  indicates the Jacobian matrix of the transformation in (1), while the symbol  $\det$  and the superscripts  $-1$  and  $-T$  denote the determinant,

the inverse, and the inverse transpose, respectively. From (2c), it is evident that, in order for the resulting transformation medium to exhibit loss and/or gain, the coordinate transformation in (1) must be complex valued. Complex-coordinate extensions of TO have already been explored in connection with single-negative transformation media [24] and field-amplitude control [25]. In the present investigation, although the framework can deal in principle with general (asymmetrical, unbalanced) loss-gain configurations, we focus on transformation media characterized by balanced loss and gain obeying the  $\mathcal{PT}$ -symmetry conditions.

First, it can be shown (see Ref. [26] for details) that the necessary condition  $n(-\mathbf{r}) = n^*(\mathbf{r})$ , usually considered in the scalar case to achieve  $\mathcal{PT}$  symmetry, can be generalized to our vector scenario as:  $\underline{\varepsilon}(-\mathbf{r}) = \underline{\varepsilon}^*(\mathbf{r})$  [or, equivalently,  $\underline{\mu}(-\mathbf{r}) = \underline{\mu}^*(\mathbf{r})$ ]. From (2c), we observe that such conditions are automatically fulfilled if the coordinate transformation in (1) is chosen so that

$$\underline{\Lambda}(-\mathbf{r}) = \underline{\Lambda}^*(\mathbf{r}). \quad (3)$$

Similar to the scalar case [2], the condition in (3) is in general not sufficient to guarantee a real eigenspectrum. As a matter of fact, beyond a critical non-Hermiticity threshold an abrupt phase transition (usually referred to as “spontaneous  $\mathcal{PT}$ -symmetry breaking”) may occur for which the eigenspectrum becomes (partially or entirely) complex (see Ref. [26] for details). It can be shown (see Ref. [26] for details) that a TO-based “ $\mathcal{PT}$  metamaterial” generated via a continuous coordinate transformation (1) [subject to (3)] from the auxiliary vacuum space is inherently characterized by full  $\mathcal{PT}$  symmetry; i.e., it does not undergo spontaneous symmetry breaking. Accordingly, this also implies that spontaneous  $\mathcal{PT}$ -symmetry breaking phenomena may be attained via suitably designed discontinuous coordinate transformations.

Our proposed TO framework allows the systematic synthesis [via (2c) and (3)] of  $\mathcal{PT}$  metamaterials, as well as the analytical modeling of their EM response [via (2a) and (2b)] and its physical interpretation in terms of analytically continued complex-coordinate wave objects residing in the auxiliary vacuum space. In what follows, for simplicity and without loss of generality, we focus on the two-dimensional (2D) scenario illustrated in Fig. 1, featuring a slab-type configuration associated with the coordinate transformation

$$x' = xu(z), \quad y' = yv(z), \quad z' = w(z), \quad |z| \leq d, \quad (4)$$

with the identity transformation implicitly assumed for  $|z| > d$  (i.e., outside the slab region).

As a first example of application, we illustrate a TO-based  $\mathcal{PT}$ -metamaterial realization of the complex source point originally pioneered by Deschamps [27] and Felsen [28] during the 1970s, and widely utilized to construct new classes of exact field solutions which convert point-

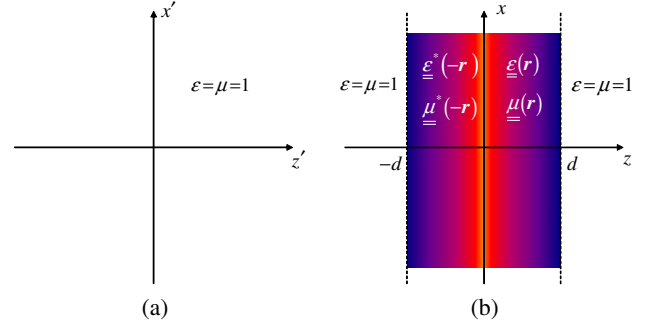


FIG. 1 (color online). Problem schematic. (a) Auxiliary vacuum space. (b) Physical space with  $\mathcal{PT}$ -metamaterial slab, of thickness  $2d$ , associated with the coordinate transformations in (4).

line-source-excited fields in a given environment into fields excited by Gaussian-beam-like wave objects in the same environment. In our example, we consider a unit-amplitude (V/m),  $y$ -directed magnetic line source centered at  $x' = 0$  with a purely imaginary displacement along the  $z'$  axis,

$$M'_y(x', z') = \delta(x')\delta(z' - ib), \quad b > 0, \quad (5)$$

for which the  $y$ -directed radiated magnetic field can be obtained via analytic continuation of the well-known 2D Green's function [29]

$$H'_y(x', z') = -\frac{\omega\varepsilon_0}{4} H_0^{(1)}(k_0 \tilde{s}'), \quad (6)$$

where  $H_0^{(1)}$  denotes the zeroth-order Hankel function of first kind,  $k_0 = \omega\sqrt{\varepsilon_0\mu_0} = 2\pi/\lambda_0$  is the vacuum wave number (with  $\lambda_0$  denoting the corresponding wavelength), and  $\tilde{s}' = \sqrt{x'^2 + (z' - ib)^2}$ ,  $\text{Re}(\tilde{s}') \geq 0$ , represents a complex distance. This particular choice of branch cut yields the so-called source-type solutions [28], associated with an equivalent source distribution occupying the region  $|x'| < b$  in the real  $z' = 0$  plane, and discontinuous across the same plane. This generates a wave object that, within the paraxial regime (near the  $z'$  axis), is well approximated by a Gaussian beam with diffraction length  $b$  propagating in the  $z' > 0$  half-space, with only weak radiation for  $z' < 0$  (see Ref. [26] for details).

Here, we show that this radiation phenomenon may be envisioned and realized in a physically appealing TO-based  $\mathcal{PT}$ -metamaterial slab excited by a line source placed in a real-coordinate point. This is based on a simple coordinate transformation (see Ref. [26] for details)

$$u(z) = v(z) = 1, \quad (7a)$$

$$w(z) = ib \left( 1 \mp \frac{z}{d} \right), \quad \text{Re}(z) \geq 0, \quad |z| \leq d, \quad \text{Im}(z) = 0^+, \quad (7b)$$

which fulfills the conditions in (3) [26], and transforms [via (2b)] the original complex line-source (radiating in vacuum) into a conventional (real-coordinate) line source embedded in a piecewise homogeneous  $\mathcal{PT}$ -metamaterial

slab occupying the region  $|z| \leq d$ . For the assumed transverse-magnetic polarization, the relevant nonzero constitutive-tensor components are purely imaginary,

$$\varepsilon_{xx} = \mu_{yy} = \mp \frac{ib}{d}, \quad \varepsilon_{zz} = \pm \frac{id}{b}, \quad z \geq 0, \quad |z| \leq d, \quad (8)$$

thereby representing a uniaxial zero-permittivity and zero-permeability metamaterial with balanced loss and gain. Note that, since the coordinate transformation in (7b) is continuous, the metamaterial slab in (8) exhibits full  $\mathcal{PT}$  symmetry. We stress that the chosen configuration serves only for illustrating, in the possibly simplest and more direct fashion, the general concept of metamaterial-induced wave field “complexification,” which is a rather broad paradigm with a wealth of deep implications. Within this framework, no attempt was made to optimize the geometry and parameters so as to ensure the practical feasibility in a specific application scenario. Nonetheless, in Ref. [26], we do address some implementation and practical feasibility issues in connection with the “exotic” media described in (8). The final result is a metamaterial that, when excited by a line source, produces the exact beam field distribution originally described by Deschamps [27] and Felsen [28] as a complex line source.

As an illustrative example, Fig. 2 shows the field map and representative cuts induced by a line source embedded in a  $\mathcal{PT}$ -metamaterial slab as in (8), with relevant parameters given in the caption. For independent verification, we compare the theoretical TO-based predictions [cf. (2a) with (6)] with results from full-wave numerical simulations (see Ref. [26] for details) which also account for the finite extent (along  $x$ ) of the slab. As it can be observed, the agreement is very good, apart for some small numerical oscillations of the phase in a region where the field amplitude is negligibly small. From a physical viewpoint, these

results nicely illustrate how the  $\mathcal{PT}$ -metamaterial slab can physically implement the complex-source displacement, reproducing at its interfaces  $z = \pm d$  the two branches of a discontinuous equivalent source distribution in the real  $z' = 0$  plane, continuously transitioning between them.

As a second illustrative example of the relevance of this complex-coordinate TO paradigm, we present a metamaterial slab supporting “anisotropic transmission resonances” for which, at a single frequency, zero reflection (with no phase accumulation) occurs only for incidence from one side of the structure and not from the other. Although these exotic propagation effects may be attained in more general non-Hermitian media (see, e.g., the Darboux-transformation approach [30]), they have recently elicited significant attention within the  $\mathcal{PT}$ -symmetry context [9–15], and have been associated with symmetry-breaking phenomena. Accordingly, we consider a coordinate transformation as in (4) [subject to (3)] with a generally discontinuous character

$$\begin{aligned} u(z) &= u_0^*, & v(z) &= v_0^*, & w(z) &= w_0^* z, & -d \leq z < 0, \\ u(z) &= u_0, & v(z) &= v_0, & w(z) &= w_0 z, & 0 < z \leq d, \end{aligned} \quad (9)$$

which yields a  $\mathcal{PT}$ -metamaterial slab as in Fig. 1. We consider a plane-wave illumination along the  $z$  axis, with  $y$ -directed magnetic field

$$H_{iy}^{(l,r)}(z) = \exp(\pm ik_0 z), \quad (10)$$

with the  $l, r$  superscripts denoting incidence from left and right (i.e.,  $+$  and  $-$  sign in the exponential), respectively. It is possible to analytically calculate the slab response by following the approach in Ref. [24] (see Ref. [26] for details). In particular, labeling  $H_{ry}^{(l,r)}$  and  $H_{ly}^{(l,r)}$  the corresponding reflected and transmitted fields, respectively, we focus on the reflection ( $R_{l,r}$ ) and transmission ( $T_{l,r}$ ) coefficients for incidence from left and right,

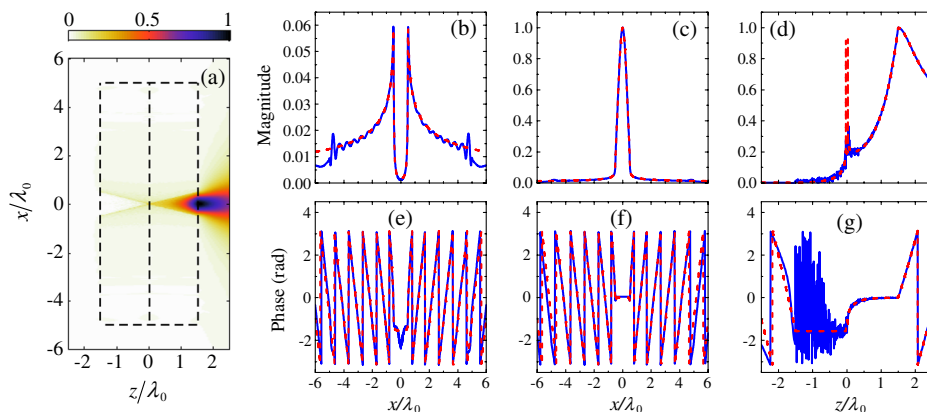


FIG. 2 (color online). (a) Numerically computed field magnitude ( $|H_y|$ ) map pertaining to a  $\mathcal{PT}$  metamaterial slab of thickness  $2d = 3\lambda_0$ , transverse width  $10\lambda_0$  (see dashed lines), and constitutive parameters as in (8) with  $b = \lambda_0/2$  (i.e.,  $\varepsilon_{xx} = \mu_{yy} = \mp i/3$ ,  $\varepsilon_{zz} = \pm 3i$ ,  $z \geq 0$ ), excited by a magnetic line source located at  $x = z = 0$ . (b), (c), (d) Transverse and longitudinal magnitude cuts (blue solid curves) at  $z = \mp(d + \Delta)$  and  $x = \Delta$ , respectively, with the small displacement  $\Delta = \lambda_0/100$  added so as to avoid branch-point and source-related singularities. (e), (f), (g) Corresponding phase profiles. Also shown (red dashed curves) are the TO-based theoretical predictions [infinite slab; cf. (2a) with (6)]. All field quantities are normalized with respect to  $H_y(0, d)$ .

$$R_l \equiv \frac{H_{ry}^{(l)}(-d)}{H_{iy}^{(l)}(-d)}, \quad R_r \equiv \frac{H_{ry}^{(r)}(d)}{H_{iy}^{(r)}(d)}, \quad (11a)$$

$$T_l \equiv \frac{H_y^{(l)}(d)}{H_{iy}^{(l)}(-d)} = T_r \equiv \frac{H_y^{(r)}(-d)}{H_{iy}^{(r)}(d)}. \quad (11b)$$

It can be shown (see Ref. [26] for details) that a sufficient condition for zero reflection and no-phase accumulation for incidence from left ( $R_l = 0$ ,  $T_l = 1$ ) is

$$v_0 = u_0 \left[ i \tan\left(\frac{w_0 k_0 d}{2}\right) \right]^{\pm 1}, \quad (12)$$

where the  $\pm 1$  exponent identifies two distinct solutions. Under these conditions, we obtain for the reflection coefficient from right [26]

$$R_r = \mp 4i \text{Im}[\cos(w_0 k_0 d)]. \quad (13)$$

The relationships above depend in a remarkably simple fashion on the transformation parameters  $u_0$ ,  $v_0$ , and  $w_0$  in (9) and the electrical thickness  $k_0 d$ , and provide useful insights into the effect of the complex-coordinate mapping. We note from (12) that solutions may exist only if  $v_0 \neq \pm u_0$ , which confirms the anticipated discontinuous character of the transformation. As expected, for a *real* coordinate transformation, solutions may exist only for complex values of the electrical thickness  $k_0 d$ , which are not physical. Similar to the previous complex-source example, our complex-coordinate TO approach allows straightforward mapping of these physically inaccessible solutions onto excitable resonant modes in a physical (real-coordinate) space. More specifically, for a given (real-valued) electrical thickness  $k_0 d$  and a desired value of the

reflection coefficient from the right ( $R_r$ ), we can obtain from (13) the required value of  $w_0$  and subsequently, from (12), the ratio  $v_0/u_0$  which identifies a continuous infinity of possible solutions. In particular, it is evident from (13) that, in order to attain *unidirectional* zero reflection (i.e.,  $R_r \neq 0$ ) the transformation parameter  $w_0$  needs simply to have non-zero real and imaginary parts.

Also in this case, the arising transformation medium is a piecewise homogeneous  $\mathcal{PT}$ -metamaterial slab,

$$\begin{aligned} \varepsilon_{xx} &= \frac{v_0^* w_0^*}{u_0^*}, & \varepsilon_{zz} &= \frac{v_0^* u_0^*}{w_0^*}, & \mu_{yy} &= \frac{u_0^* w_0^*}{v_0^*}, & -d \leq z < 0, \\ \varepsilon_{xx} &= \frac{v_0 w_0}{u_0}, & \varepsilon_{zz} &= \frac{v_0 u_0}{w_0}, & \mu_{yy} &= \frac{u_0 w_0}{v_0}, & 0 < z \leq d, \end{aligned} \quad (14)$$

which, for the assumed polarization, can be made effectively nonmagnetic (i.e.,  $\mu_{yy} = 1$ ) by enforcing  $u_0 w_0 = v_0$ , and isotropic ( $\varepsilon_{xx} = \varepsilon_{zz}$ ) by enforcing  $u_0 = \pm w_0$ . This significantly simplifies the practical implementation, at the expense of reducing the degrees of freedom in the solutions, which are now related to the (countably infinite, for given  $k_0 d$ ) roots of the transcendental equations

$$w_0 = \left[ i \tan\left(\frac{w_0 k_0 d}{2}\right) \right]^{\pm 1}, \quad (15)$$

without direct control of  $R_r$  in (13).

Figure 3 shows the numerically computed [26] field maps and relevant field cuts (blue solid curves) for a Gaussian-beam exciting a nonmagnetic, isotropic, truncated  $\mathcal{PT}$ -metamaterial slab with moderate thickness ( $2d = 4\lambda_0$ ) and  $\varepsilon_{xx} = \varepsilon_{zz} = 3.079 \mp 0.359i$ ,  $z \geq 0$ . It is fairly

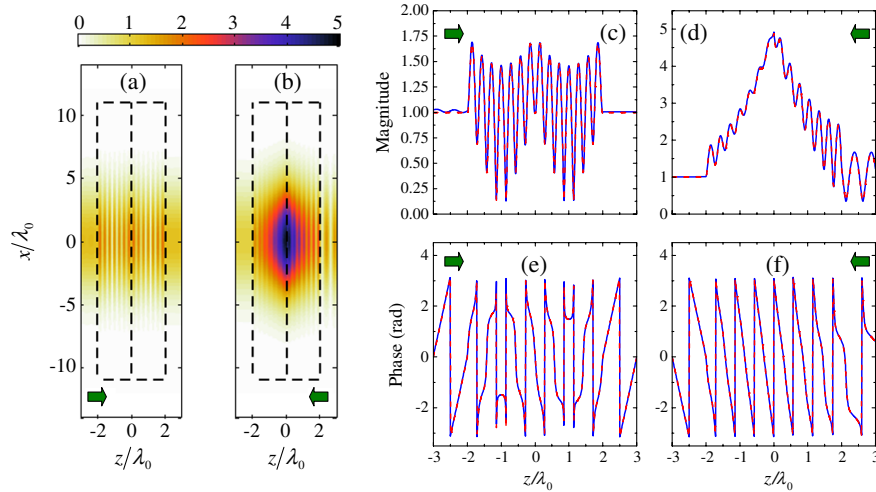


FIG. 3 (color online). (a), (b) Numerically-computed field magnitude ( $|H_y|$ ) maps pertaining to a  $\mathcal{PT}$ -metamaterial slab of thickness  $2d = 4\lambda_0$ , transverse width  $22\lambda_0$  (see dashed lines), and constitutive parameters as in (8) with  $u_0 = w_0 = 1.758 - 0.102i$  and  $v_0 = 3.079 - 0.359i$  (i.e.,  $\varepsilon_{xx} = \varepsilon_{zz} = 3.079 \mp 0.359i$ ,  $z \geq 0$ , and  $\mu_{yy} = 1$ ), excited by a unit-amplitude Gaussian beam with minimum waist of  $4\lambda_0$  normally-incident from left and right, respectively (as schematically indicated by the thick arrows). (c), (d) Magnitude cuts (blue solid curves) along the beam axis ( $x = 0$ ), for incidence from left and right, respectively. (e), (f) Corresponding phase profiles. Also shown (red dashed curves) are the TO-based theoretical predictions (infinite slab and plane-wave incidence) [26].

evident the strong difference between the responses pertaining to incidence from the left [nearly-zero reflection with no phase accumulation; cf. Figs. 3(a), 3(c), and 3(e)] and right [sensible reflection ( $|R_r| \approx 0.67$ ); cf. Figs. 3(b), 3(d), and 3(f)]. Once again, these results are in very good agreement with the TO-based theoretical predictions (red dashed curves) for infinite slab and plane-wave excitation. Also in this case, the parameters were mainly chosen for the sake of simplicity of illustration and visualization, and the resulting gain levels required turn out to be unrealistic within current technology. However, we did verify that, in line with similar scenarios in the literature [15], much more feasible levels of loss or gain may be traded off for larger electrical-thickness values (see Ref. [26] for details). Finally, a detailed study of the spontaneous symmetry-breaking phenomenon can be found in Ref. [26].

In conclusion, we have shown that complex-coordinate TO may be exploited for systematic generation, design, and modeling of  $\mathcal{PT}$  metamaterials for a variety of applications. As illustrated in our examples, the most attractive and interesting aspect of the proposed approach is the metamaterial-based transposition to an actual physical space of wave objects and resonant states residing in complex-coordinate spaces. Given the power and pervasiveness of analytic-continuation approaches in wave physics, this is expected to open up a plethora of new intriguing venues for  $\mathcal{PT}$  metamaterials. Accordingly, current and future studies are aimed at exploring more general transformation classes, as well as different geometries (e.g., cylindrical and spherical) and applications.

A. A. acknowledges the support of Dr. Arje Nachman under the AFOSR YIP Grant No. FA9550-11-1-0009.

---

\*vgaldi@unisannio.it

- [1] C. M. Bender and S. Boettcher, *Phys. Rev. Lett.* **80**, 5243 (1998).
- [2] C. M. Bender, *Rep. Prog. Phys.* **70**, 947 (2007).
- [3] S. Xiao, V. P. Drachev, A. V. Kildishev, X. Ni, U. K. Chettiar, H.-K. Yuan, and V. M. Shalaev, *Nature (London)* **466**, 735 (2010).
- [4] K. G. Makris, R. El-Ganainy, D. N. Christodoulides, and Z. H. Musslimani, *Phys. Rev. Lett.* **100**, 103904 (2008).
- [5] M. C. Zheng, D. N. Christodoulides, R. Fleischmann, and T. Kottos, *Phys. Rev. A* **82**, 010103(R) (2010).
- [6] A. Guo, G. J. Salamo, D. Duchesne, R. Morandotti, M. Volatier-Ravat, V. Aimez, G. A. Siviloglou, and D. N. Christodoulides, *Phys. Rev. Lett.* **103**, 093902 (2009).
- [7] C. E. Rüter, K. G. Makris, R. El-Ganainy, D. N. Christodoulides, M. Segev, and D. Kip, *Nat. Phys.* **6**, 192 (2010).
- [8] A. A. Sukhorukov, Z. Y. Xu, and Y. S. Kivshar, *Phys. Rev. A* **82**, 043818 (2010).
- [9] H. Ramezani, T. Kottos, R. El-Ganainy, and D. N. Christodoulides, *Phys. Rev. A* **82**, 043803 (2010).
- [10] S. Longhi, *Phys. Rev. A* **81**, 022102 (2010).
- [11] Z. Lin, H. Ramezani, T. Eichelkraut, T. Kottos, H. Cao, and D. N. Christodoulides, *Phys. Rev. Lett.* **106**, 213901 (2011).
- [12] S. Longhi, *J. Phys. A* **44**, 485302 (2011).
- [13] Li Ge, Y. D. Chong, and A. D. Stone, *Phys. Rev. A* **85**, 023802 (2012).
- [14] A. Regensburger, C. Bersch, M.-A. Miri, G. Onishchukov, D. N. Christodoulides, and U. Peschel, *Nature (London)* **488**, 167 (2012).
- [15] A. Mostafazadeh, *Phys. Rev. A* **87**, 012103 (2013).
- [16] A. Mostafazadeh, *Phys. Rev. Lett.* **102**, 220402 (2009).
- [17] S. Longhi, *Phys. Rev. A* **82**, 031801(R) (2010).
- [18] Y. D. Chong, Li Ge, and A. D. Stone, *Phys. Rev. Lett.* **106**, 093902 (2011).
- [19] U. Leonhardt, *Science* **312**, 1777 (2006).
- [20] J. B. Pendry, D. Schurig, and D. R. Smith, *Science* **312**, 1780 (2006).
- [21] H. Chen, C. T. Chan, and P. Sheng, *Nat. Mater.* **9**, 387 (2010).
- [22] G. Lévai and M. Znojil, *J. Phys. A* **33**, 7165 (2000).
- [23] M. Znojil and G. Lévai, *Phys. Lett. A* **271**, 327 (2000).
- [24] G. Castaldi, I. Gallina, V. Galdi, A. Alù, and N. Engheta, *J. Opt.* **13**, 024011 (2011).
- [25] B.-I. Popa and S. A. Cummer, *Phys. Rev. A* **84**, 063837 (2011).
- [26] See Supplemental Material at <http://link.aps.org/supplemental/10.1103/PhysRevLett.110.173901> for details on analytical and numerical calculations, and for additional results.
- [27] G. A. Deschamps, *Electron. Lett.* **7**, 684 (1971).
- [28] L. B. Felsen, Symposia on theoretical Physics and mathematics **18**, 39 (1976).
- [29] L. B. Felsen and N. Marcuvitz, *Radiation and Scattering of Waves* (IEEE-Wiley, Piscataway, NJ, 1994).
- [30] S. Longhi, *Phys. Rev. A* **82**, 032111 (2010).